AEROSOL REMOTE SENSING WITH AATSR: A DUAL-VIEW OPTIMAL ESTIMATION SURFACE BRDF RETRIEVAL SCHEME

A. M. Sayer[1], G. E. Thomas[1], R. G. Grainger[1], C. T. Mutlow[2]

1. Atmospheric, Oceanic and Planetary Physics, Department of Physics, University of Oxford
2. Rutherford Appleton Laboratory, Chilton, Didcot, Oxfordshire

sayer@atm.ox.ac.uk

INTRODUCTION

The differing path lengths of AATSR's forward and nadir views can be used to separate the contributions from aerosol scattering and surface reflectance in the observed top-of-atmosphere (TOA) radiance. This poster presents an extension of the nadir-view Oxford-RAL retrieval of Aerosols and Clouds (ORAC) scheme used by the GRAPE and GlobAEROSOL projects (Thomas *et al.*, 2007) to take advantage of the dual-view capabilities AATSR offers, using a new surface BRDF forward model (Thomas, 2007).

The new algorithm uses optimal estimation to retrieve aerosol optical depth at 550 nm, effective radius and the white-sky surface albedo at AATSR visible channel wavelengths.

Retrieval results for the month of September 2004, with a comparison of optical depth against AERONET measurements, are also presented.

INSTRUMENTAL DETAILS

The Advanced Along-Track Scanning Radiometer (AATSR) aboard Envisat, launched March 2002, is the successor of the earlier similar instruments ATSR and ATSR-2. It measures TOA reflectance at 7 wavelengths in the visible and IR, the first four of which (550 nm, 660 nm, 870 nm and 1.6 µm) are used in the aerosol retrieval.

A special feature of the instruments is their two viewing geometries. They obtain forward-view measurements at a zenith angle of 53°-55°, and around 100 seconds later sample the same region at a nadir viewing zenith angle of 0°-22°.

The swath width is 512 km meaning global coverage is achieved every 3 days. Ground pixel resolution is approximately 1 km by 1 km for the nadir view and 1.5 km by 1.5 km for the forward; as a result the retrieval is normally performed at 3 km by 3 km resolution. This 'superpixelling' to a lower resolution additionally decreases the effect of instrumental noise.

RETRIEVAL ALGORITHM

ORAC is an optimal estimation (OE) retrieval (Rodgers, 2000) employing Levenburg-Marquardt iteration to find a solution. The rigorous statistical basis of the OE scheme provides the following advantages:

1. Estimates of error on individual retrieved parameters
2. Quality control on the solution (retrieval 'cost')
3. Assimilation of *a priori* information on the surface and atmospheric state

The measurement vector y_m consists of 8 measurements of TOA radiance (4 channels at two geometries). From this we retrieve:

1. Aerosol optical depth τ at 550 nm.
2. Distribution effective radius r_e. Together with $\tau_{(550)}$ this can be used to obtain the optical depth at 870 nm and the Ångstrom exponent between these two wavelengths.
3. The white-sky albedo of the surface at 550 nm, 660 nm, 870 nm and 1.6 µm.

REFERENCES

A. Birks, Improvements to the AATSR IPF relating to land surface temperature, *ESA Technical Note*, 2004

A. Birks and ESA, AATSR Product Handbook, version 2.2, 2007, *http://envisat.esa.int/handbooks/aatsr/*

J. Brown, M. Hoke, K. Doherty, G. Anderson, A. Berk, MODTRAN 4 software, 2004, *http://www.vs.afrl.af.mil/ProductLines/IRClutter/modtran4.aspx*

C.S. Cox, W.H. Munk, Measurement of the roughness of the sea surface from photographs of the Sun's glitter, *J. Opt. Soc. Am.*, 1954*a*, **44**, 838-850.

C.S. Cox, W.H. Munk, Statistics of the sea surface derived from Sun glitter, *J. Mar. Res.*, 1954*b*, **13**, 198-227.

O. Dubovik, B. Holben, T.F. Eck, A. Smirnov, Y.J. Kaufman, M.D. King, D. Tanré, I. Slutsker, Variability of absorption and optical properties of key aerosol types observed in worldwide locations, *J.Atm.Sci.*, 2002, **59**, 590–608

M. Hess, P. Koepke, I. Schult, Optical properties of aerosols and clouds: The software package OPAC, *Bull. Am. Met. Soc.*, 1998, **79**(5), 831-944.

C.D. Rodgers, Inverse methods for atmospheric sounding: Theory and Practice, 2000, *World Scientific.*

K. Stamnes, S-C. Tsay, W. Wiscombe, K. Jayaweera, Numerically stable algorithm for discrete-ordinate-method radiative transfer in multiple scattering and emitting layer media, *Appl. Opt.*, 1988, **27**(12), 2502-2509.

G.E. Thomas, S.H. Marsh, S.M.Dean, E.Carboni, R.G.Grainger, C.A.Poulsen, R.Siddans, B.J. Kerridge, An optimal estimation retrieval scheme for (A)ATSR, *AOPP Memorandum 2007.1*, 2007.

A. M. Sayer, A sea surface reflectance model suitable for use with AATSR aerosol retrieval, *AOPP Memorandum, 2007.2*, 2007

G.E. Thomas, A surface BRDF forward model for ORAC, *AOPP Memorandum, 2007.3*, 2007

W. Wanner, A.H. Strahler, B. Hu, P. Lewis, J.-P. Muller, X. Li, X., Schaaf, C.L. Barker, M.J. Barnsley, Global retrieval of bidirectional reflectance and albedo over land from EOS MODIS and MISR data: Theory and algorithm, *J. Geophys. Res.*, 1997.

AEROSOL MODEL

Aerosol microphysical properties from the OPAC database (Hess *et al.*, 1998) have been used to generate aerosol models corresponding to typical continental, maritime, dust and urban aerosol. Additionally, Dubovik *et al.* (2002) has been used to generate a biomass burning aerosol class. Each class consists of up to 4 aerosol components, represented by lognormal distributions with differing modal radius and spread. Size distributions with different effective radii are obtained by altering the mixing ratio of these components. These classes are then fed into the atmospheric forward model.

ATMOSPHERIC FORWARD MODEL

The purpose of the forward model is to predict TOA radiance given atmospheric and surface conditions. The aerosol class models are used with the DISORT radiative transfer code (Stamnes *et al.*, 1988) and MODTRAN gas absorption database (Brown *et al.*, 2004) to generate lookup tables (LUTs) of atmospheric transmission and reflectance over a range of geometric and aerosol (varying optical depth and effective radius) conditions. Additionally, three different surface reflectances are defined:

1. The bidirectional reflectance of the surface, R_{SBD}. This makes use of *a priori* information dependent on the pixel type, and is defined by a bidirectional reflectance distribution function (BRDF). Land pixels use the MODIS land surface reflectance product (Wanner *et al.*, 1997), while over the ocean a model (Sayer, 2007) based on Cox and Munk (1954*a,b*) wave statistics and pigment concentrations is employed.
2. The black-sky albedo, R_{SB}. This is obtained by integration of the bidirectional reflectance over all satellite zenith and relative azimuth angles. It represents the scattering of a direct beam of light over a hemisphere.
3. The white-sky albedo, R_{SW}. This is obtained by integration of the black-sky albedo over all solar angles, and hence has no geometric dependence.

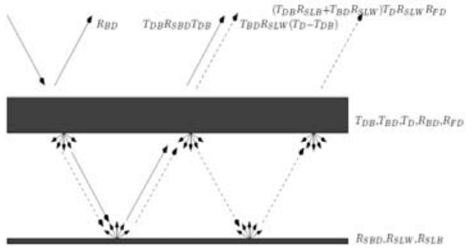

Figure 1: Surface-atmosphere interactions in the forward model. Taken from Thomas (2007).

Multiple scattering between the surface and atmosphere as shown in Figure 1 is used to predict the total TOA radiance, according to Equation 1. The R_X and T_X represent the reflectance or transmittance of the atmosphere to direct and diffuse radiation, and are functions of geometry and aerosol properties.

$$R = R_{BD} + T_{DB}\left(R_{SBD} - R_{SB}\right)T_{DB} + \frac{\left(T_{DB}R_{SB} + T_{BD}R_{SW}\right)T_D}{1 - R_{SW}R_{FD}}$$

Equation 1: TOA radiance

During the retrieval, the ratio between the BRDF, black-sky albedo and white-sky albedo, as set by MODIS data over land and the model of Sayer (2007) over ocean, is fixed.

ITERATION AND QUALITY CONTROL

Starting from a first guess at the atmospheric state x, set equal to the *a priori* values x_b, linear interpolation of the LUTs is used to give a first estimate of TOA radiance. This is compared to the observed values y_m and iteration proceeds via a weighted combination of steepest descent and Newtonian iteration (the Levenburg-Marquadt method). The solution is found based on the minimisation of a cost function, J (Equation 2). This is a least-squares fit of the measurements, weighted by the uncertainty on them (S_y) and *a priori* values (S_x). A maximum of 25 iterations are permitted before iteration is abandoned; failure to converge is noted.

$$J = \left(y(x) - y_m\right)S_y^{-1}\left(y(x) - y_m\right)^T + \left(x - x_b\right)S_x^{-1}\left(x - x_b\right)^T$$

Equation 2: The cost function

The retrieval is not performed in case of cloud cover. The ESA cloud flag (Birks *et al.*, 2007) is used over the ocean and the algorithm of Birks (2004) is used over the land.

SEPTEMBER 2004 RESULTS

AATSR data for the month of September 2004 has been processed with the dual-view retrieval algorithm. Monthly mean products are shown in Figure 2. Gaps are generally due to cloud cover, or low retrieval quality due to bright (desert or ice) surfaces. Future developments will improve retrievals over bright surfaces.

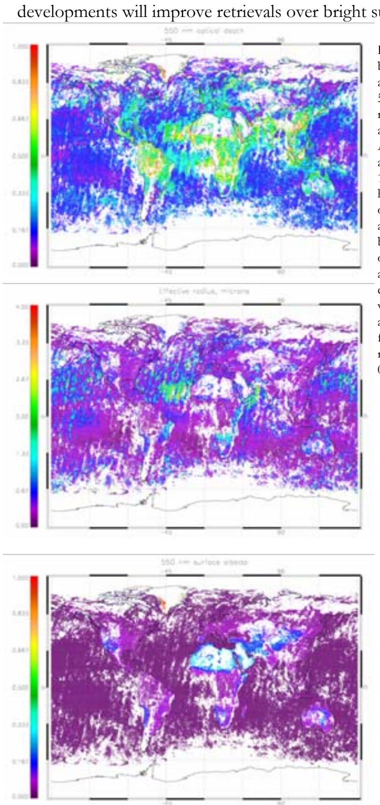

Figure 2: From top – bottom: Retrieved aerosol optical depth at 550 nm, effective radius, and surface albedo at 550 nm. Albedo is also retrieved at 660 nm, 870 nm and 1600 nm but omitted here for brevity. The optical depth at 550 nm and effective radius may be used to calculate an optical depth at 870 nm and the Ångstrom exponent between these wavelengths. All data are monthly mean plots for September 2004, retrieved on a 0.2° x 0.2° grid.

Aerosol speciation is shown in Figure 3. Speciation is currently determined via a brute-force method: the aerosol model resulting in a retrieval with the lowest cost (Equation 2) sets the aerosol type.

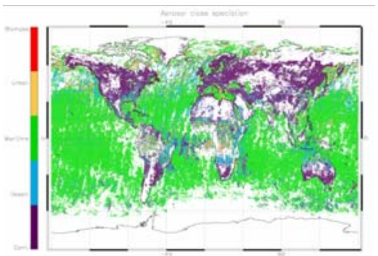

Figure 3: Speciation of aerosol into one of the five different aerosol classes used in the retrieval: continental, dust, maritime, urban and biomass burning.

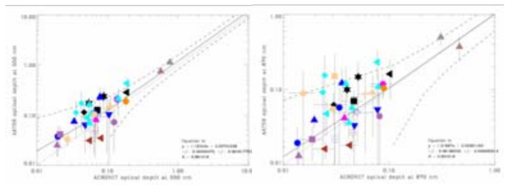

Figure 4: Comparison of retrieved AATSR optical depth at 550 nm (left) and 870 nm (right) with ground-based AERONET measurements. Different symbols correspond to different AERONET stations, with brighter colours indicating brighter land surfaces. Matches were made between AATSR and clear-sky ground measurements within 30 minutes of an Envisat overpass.

AERONET VALIDATION

Validation of speciated aerosol optical depth at both 550 nm and 870 nm with AERONET within 30 minutes of satellite overpasses is shown in Figure 4. Correlation coefficients are very good (0.96 at 550 nm and 0.82 at 870 nm) and the gradient of the line of best fit is close to 1 with a small intercept in both cases. AERONET is thanked for providing the ground truth data.

RELATED POSTERS

- Carboni *et al.*, poster 009,*Retrieval of desert dust from visible and infrared SEVIRI data*
- Poulsen *et al.*, poster 094, *Cloud and aerosol climatologies from A/ATSR, SEVIRI and MERIS*

ONLINE

- **ORAC:** *http://www.atm.ox.ac.uk/project/ORAC/*
- **GRAPE:** *http://www.atm.ox.ac.uk/project/grape/*
- **GlobAerosol:** *http://www.atm.ox.ac.uk/project/Globaerosol* and *http://www.globaerosol.info*